

Magnetic microstructure in a stress-annealed Fe_{73.5}Si_{15.5}B₇Nb₃Cu₁ soft magnetic alloy observed using off-axis electron holography and Lorentz microscopy

A. Kovács^{*}, K. G. Pradeep, G. Herzer, D. Raabe, and R. E. Dunin-Borkowski

Citation: *AIP Advances* **6**, 056501 (2016); doi: 10.1063/1.4942954

View online: <http://dx.doi.org/10.1063/1.4942954>

View Table of Contents: <http://aip.scitation.org/toc/adv/6/5>

Published by the *American Institute of Physics*

Articles you may be interested in

[Quantitative extraction of in-plane surface properties using torsional resonance mode of atomic force microscopy](#)

AIP Advances **97**, 083533083533 (2005); 10.1063/1.1876576

[A uniaxial tensile stress apparatus for temperature-dependent magnetotransport and optical studies of thin films](#)

AIP Advances **73**, (2002); 10.1063/1.1516852

[Nonmagnetic semiconductors as read-head sensors for ultra-high-density magnetic recording](#)

AIP Advances **80**, (2002); 10.1063/1.1481238

[Investigation of the humidity effect on the electrical properties of single-walled carbon nanotube transistors](#)

AIP Advances **87**, 093101093101 (2005); 10.1063/1.2032594

HAVE YOU HEARD?

Employers hiring scientists and
engineers trust

PHYSICS TODAY | JOBS

www.physicstoday.org/jobs



Magnetic microstructure in a stress-annealed $\text{Fe}_{73.5}\text{Si}_{15.5}\text{B}_7\text{Nb}_3\text{Cu}_1$ soft magnetic alloy observed using off-axis electron holography and Lorentz microscopy

A. Kovács,^{1,a} K. G. Pradeep,^{2,3} G. Herzer,⁴ D. Raabe,²
 and R. E. Dunin-Borkowski¹

¹*Ernst Ruska-Centre for Microscopy and Spectroscopy with Electrons and Peter Grünberg Institute, Forschungszentrum Jülich, D-52425 Jülich, Germany*

²*Materials Chemistry, RWTH Aachen University, D-52074 Aachen, Germany*

³*Department for Microstructure Physics and Alloy Design, Max-Planck-Institut für Eisenforschung GmbH, D-40237 Düsseldorf, Germany*

⁴*Vacuumschmelze GmbH & Co KG, D-63450 Hanau, Germany*

(Presented 15 January 2016; received 6 November 2015; accepted 2 December 2015; published online 23 February 2016)

Fe-Si-B-Nb-Cu alloys are attractive for high frequency applications due to their low coercivity and high saturation magnetization. Here, we study the effect of stress annealing on magnetic microstructure in $\text{Fe}_{73.5}\text{Si}_{15.5}\text{B}_7\text{Nb}_3\text{Cu}_1$ using off-axis electron holography and the Fresnel mode of Lorentz transmission electron microscopy. A stress of 50 MPa was applied to selected samples during rapid annealing for 4 s, resulting in uniaxial anisotropy perpendicular to the stress direction. The examination of focused ion beam milled lamellae prepared from each sample revealed a random magnetic domain pattern in the sample that had been rapidly annealed in the absence of stress, whereas a highly regular domain pattern was observed in the stress-annealed sample. We also measured a decrease in domain wall width from ~ 94 nm in the sample annealed without stress to ~ 80 nm in the stress-annealed sample. © 2016 Author(s). All article content, except where otherwise noted, is licensed under a Creative Commons Attribution 3.0 Unported License. [<http://dx.doi.org/10.1063/1.4942954>]

The addition of small amounts of Cu and Nb to Fe-Si-B based amorphous alloys,¹ in combination with different heat treatment methods, results in the formation of nanocomposite microstructures with excellent soft magnetic properties.² The addition of Cu is particularly important, as it induces a high density of DO_3 structured Fe_3Si nanocrystals, which constitute the primary magnetic phase in this system.^{3–6} The crystallization onset temperature varies depending on the type of annealing and is higher (by at least 100 °C) when performing rapid annealing (RA) for a few (4–10) seconds.^{3,4,7} Depending on the desired application, the magnetic properties of the alloys can also be tailored during annealing by applying a magnetic field or a tensile stress, both of which yield uniform uniaxial anisotropy.^{2,7,8} The effect of applied stress on the structural anisotropy has been studied using transmission x-ray diffraction. It was observed that lattice spacing of certain planes show anisotropy (i.e elongation), which is proportional to the applied stress.⁹ Similarly, the effect of stress annealing on the magnetic microstructure of $\text{Fe}_{73.5}\text{Si}_{15.5}\text{B}_7\text{Nb}_3\text{Cu}_1$ ribbons has previously been studied using magneto-optical Kerr microscopy,⁷ which provides useful information about magnetic domain structure in bulk samples.

Here, we study the effect of stress annealing on the microstructure and magnetic properties of $\text{Fe}_{73.5}\text{Si}_{15.5}\text{B}_7\text{Nb}_3\text{Cu}_1$ alloys¹⁰ with high spatial resolution in the transmission electron microscope (TEM) using both the Fresnel mode of Lorentz TEM and off-axis electron holography. A 50 MPa

^acorresponding author: electronic mail a.kovacs@fz-juelich.de

stress was applied to selected samples during rapid annealing, resulting in strong uniaxial magnetic anisotropy K_u perpendicular to the stress direction, as confirmed by bulk measurements (not shown) performed using superconducting quantum interference device magnetometry both at room temperature and at 10 K. The magnetic configuration of a sample that had been rapidly annealed (RA) at 695 °C for 10 s in the absence of an applied stress was compared with that of a sample that had been stress annealed (SA) at 690 °C for 4 s. X-ray diffraction and atom probe tomography (APT)^{3,4} revealed that both annealed samples contained ~ 80 vol. % of a crystalline Fe_3Si phase with a DO_3 structure, while the remaining amorphous matrix was enriched in B, Nb and Cu precipitates. For structural and magnetic characterization, thin sections with lateral dimensions of $\sim 10 \times 10 \mu\text{m}$ were cut from the annealed ribbons and thinned to electron transparency ($\sim 100 \text{ nm}$) using an FEI Helios Nanolab 600i dual beam scanning electron microscope (SEM) equipped with a focused ion beam (FIB). Figure 1(a) shows an SEM image of a TEM lamella of SA FeSiBNbCu , which was prepared with stress direction in the plane of the specimen (see below). The advantage of FIB preparation over other methods such as electro-polishing is that the sample has a large field of view and uniform thickness. Artifacts introduced by the high energy (30 keV) Ga^+ ion beam during FIB milling were reduced by subsequent low energy (0.9 keV) Ar ion milling using a Fischione Nanomill system. Figures 1(b) and 1(c) show bright-field (BF) TEM images of the microstructure in both samples, which contain randomly oriented Fe_3Si nanocrystals. The sizes of the Fe_3Si grains and Cu precipitates are almost identical in both samples, despite the fact that the RA sample had been annealed for a few seconds longer. Corresponding selected area electron diffraction (SAED) patterns, which are shown in the insets to Figs 1(b) and 1(c), confirm the DO_3 structure and the random orientation of the Fe_3Si grains. A faint diffraction ring arising from the Nb- and B-rich matrix overlaps with the much more intense Fe_3Si 220 ring in the SAED patterns. A high-resolution TEM image shown in Fig. 1(d) reveals an amorphous matrix surrounding the crystals. The presence of ~6 nm Cu precipitates was confirmed using both APT^{3,4} and energy dispersive X-ray spectroscopy (not shown).

Figure 2 shows representative Fresnel defocus images of magnetic domain patterns in the annealed samples recorded at 300 keV in magnetic-field-free conditions in an FEI Titan TEM operated

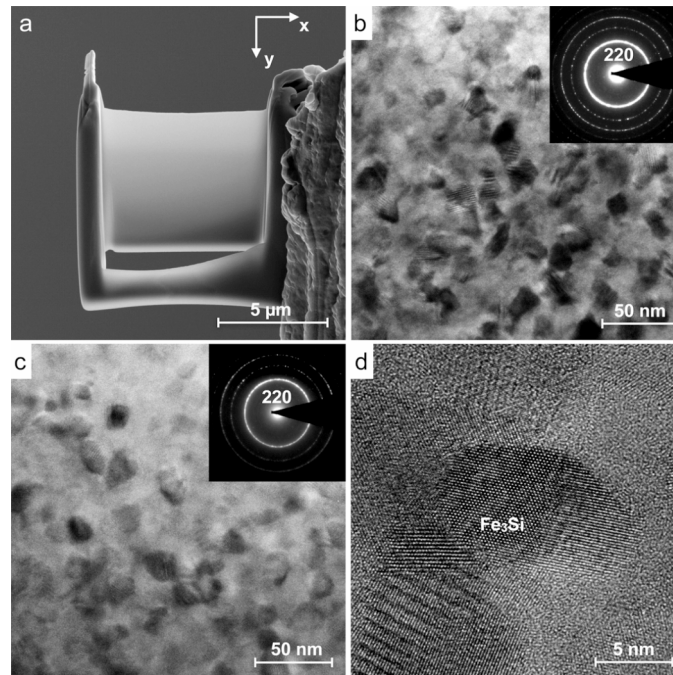


FIG. 1. (a) SEM image of a TEM specimen of SA FeSiNbCuB . The stress was applied along the x direction. (b, c) BF TEM images and SAED patterns of the RA and SA samples, which have random polycrystalline structures. (d) High-resolution TEM image of Fe_3Si grains in an amorphous Nb- and B-rich matrix. The average grain size is ~10 nm.

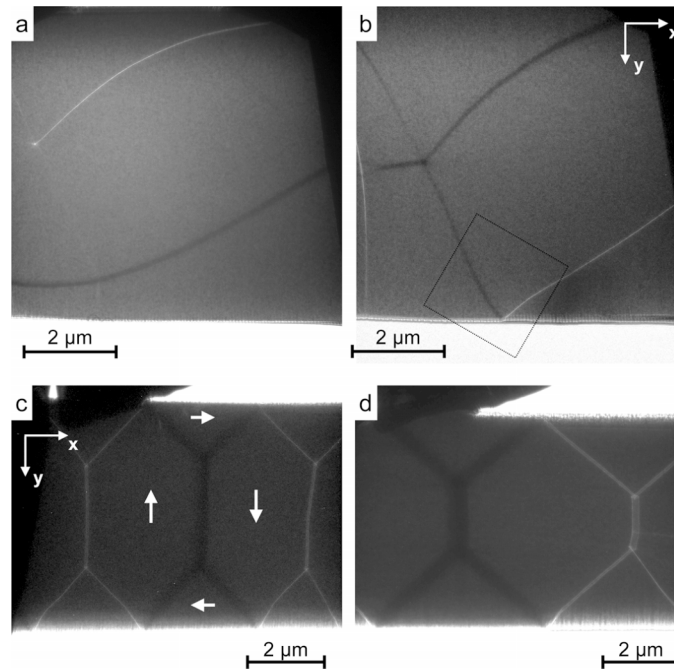


FIG. 2. Fresnel defocus images recorded in Lorentz mode from (a, b) RA and (c, d) SA FeSiBNbCu alloy samples after saturation of each specimen using an out-of-plane magnetic field. A random magnetic domain pattern is visible in the sample that had been annealed in the absence of an applied stress (a, b). The rectangle in (b) marks a region that was studied using off-axis electron holography. The (a-c) and (d) images were recorded 1 mm and 1.2 mm out of focus, respectively. The stress was applied parallel to the x direction in (c, d).

in Lorentz mode. In this imaging mode, the component of the projected magnetic flux density that lies perpendicular to the incident electron beam induces a Lorentz force, which deflects the electrons and results in convergent or divergent domain wall (DW) contrast that changes sign between under and over focus conditions. The magnetic-field-free condition for Lorentz TEM was achieved by turning off the conventional objective lens of the microscope. The objective lens could then be excited slightly in order to apply magnetic fields of up to 2.5 T to the sample, which was tilted to select the direction of the applied field relative to its plane.

In the experiments described below, a magnetic field of 1.5 T was applied perpendicular to the plane of the annealed FeSiBNbCu samples in order to saturate them magnetically, before reducing the applied field to zero and studying the resulting magnetic domain structure. The saturating magnetic field for both RA and SA samples was applied parallel to z direction in Fig. 2. Figures 2(a) and 2(b) show that the magnetic domain pattern in the RA FeSiBNbCu sample, which was not subjected to an applied stress during annealing, is fully random. The DWs are slightly curved and occasionally cross-tie walls can be observed. Despite the random orientations of the nanocrystals, a ripple-like magnetic structure was not observed. In contrast, Figs 2(c) and 2(d) show a highly regular domain pattern in the SA FeSiBNbCu sample. Adjacent magnetic domains are separated by either 180° or 90° DWs, resulting a magnetic flux closure state. The primary axes of the magnetic domains are perpendicular to the stress direction (x in Fig. 2), which is the magnetic hard axis.

Figure 3(a) shows part of an off-axis electron hologram recorded at 300 keV using a Gatan K2 IS direct electron detection camera in Lorentz mode from the RA FeSiBNbCu. The voltage applied to the electron biprism was 100 V, resulting in an interference fringe spacing of ~ 2.6 nm and a fringe contrast of $\sim 25\%$. The technique allows the projected in-plane magnetic flux density to be determined from local changes in the spacing and direction of the interference fringes.¹¹ In the present specimen, the mean inner potential contribution to the recorded signal was assumed to be uniform inside the specimen. Figure 3(b) shows the resulting magnetic induction map determined from the off-axis electron hologram, displayed using a combination of phase contours, colors and

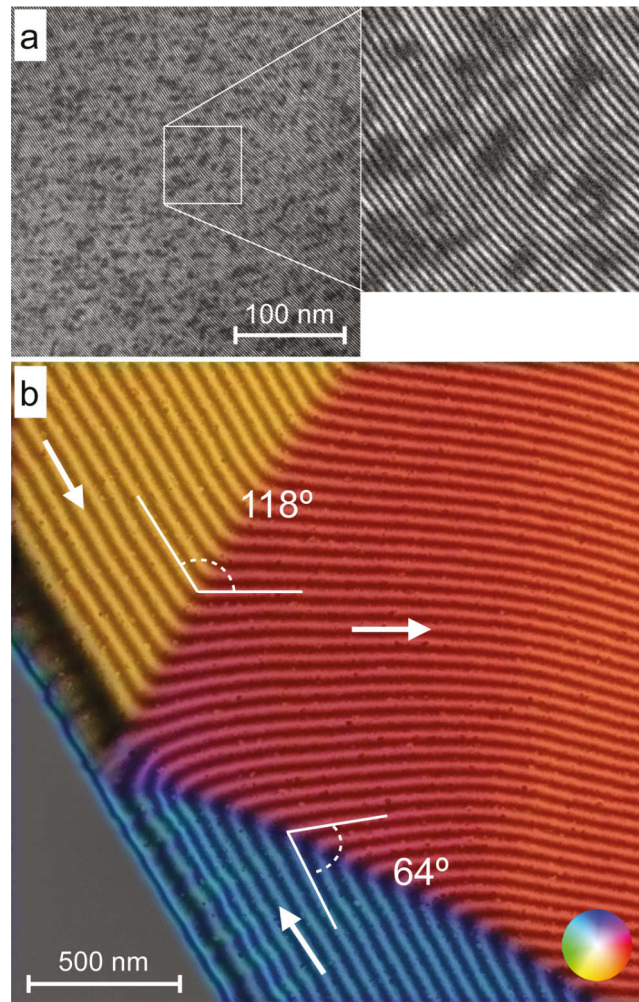


FIG. 3. (a) Off-axis electron hologram of the RA FeSiNbCuB sample recorded in focus. The small patches of dark contrast correspond to strongly diffracting Fe₃Si grains. The enlarged region shows the bending of the electron holographic interference fringes, which results from local variations in projected magnetic flux density in the specimen. (b) Magnetic induction map inferred from the region of the off-axis electron hologram from the region indicated in (a). The phase contour spacing is 2π . Local changes in magnetization direction were inferred from changes in the direction of the phase contours across DWs.

arrows. On the assumption that the measurements are not affected substantially by demagnetizing fields, the angles between adjacent domains are measured to be $118^\circ \pm 4^\circ$ and $64^\circ \pm 4^\circ$.

The magnetic properties of nanocrystalline FeSiBNbCu alloys can be described using a random anisotropy model,¹² which assumes a distribution of magnetic anisotropy axes of the randomly oriented Fe₃Si grains, with interplay between exchange and induced anisotropy energies. This model is characterized by a ferromagnetic correlation exchange length L_{ex} , which is proportional to $A/\langle K \rangle$, where A is the exchange stiffness and $\langle K \rangle$ is an effective anisotropy constant. L_{ex} corresponds to a scale below, which the direction of magnetization cannot vary. It therefore places a lower limit on the magnitude of the domain wall width.

The widths of DWs in both samples were determined by extrapolating the full width at half minimum (FWHM) of the contrast of a 180° DW measured from Fresnel defocus images as a function of defocus to zero defocus (Fig. 4). The measurements suggest a decrease in DW width from 94 ± 10 nm in the RA sample to 80 ± 10 nm in the SA sample. Preliminary measurements (not shown) indicate a further decrease in DW width in samples annealed at still higher stresses. The decrease in DW width may be explained by the tensile-stress-induced anisotropy K_u , which decreases the ferromagnetic exchange length.

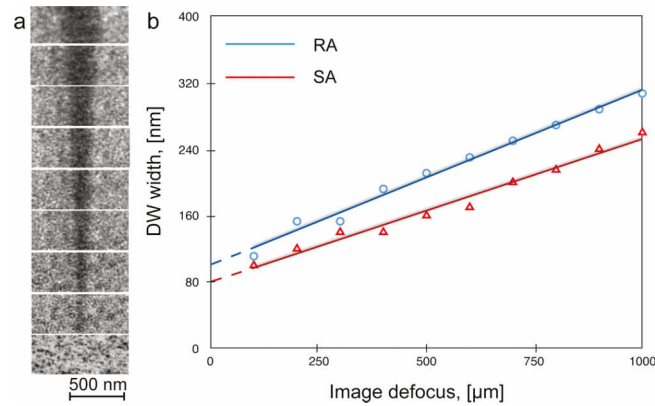


FIG. 4. (a) Fresnel defocus images of a 180° DW in the SA FeSiNbCuB sample. The defocus difference between successive images is 100 μm. (b) FWHM values of divergent DWs measured from defocus series recorded from the RA and SA FeSiNbCu samples.

In summary, the microstructure and magnetic domain states of annealed FeSiNbCu samples have been measured for samples that had been rapidly annealed in the absence and in the presence of an applied stress (creep). A highly ordered magnetic domain pattern of 180° and 90° DWs, which was observed in the stress-annealed sample, is likely to result from an increase in stress-induced uniaxial magnetic anisotropy. Experimental measurements indicate that the DW width decreases from 94 ± 10 nm to 80 ± 10 nm between the sample annealed in the absence of stress and the stress-annealed sample.

ACKNOWLEDGEMENTS

The authors would like to thank Dr. P. Choi (MPIE Duesseldorf, Germany) and Dr. M. Ohnuma (Hokkaido University, Japan) for their helpful discussions. RDB is grateful to the European Research Council for an Advanced Grant.

- ¹ Y. Yoshizawa, S. Oguma, and K. Yamauchi, *J. Appl. Phys.* **64**, 6044 (1988).
- ² G. Herzer, *Acta Materialia* **61**, 718 (2013).
- ³ K. G. Pradeep, G. Herzer, P. Choi, and D. Raabe, *Acta Materialia* **68**, 295 (2014).
- ⁴ K. G. Pradeep, G. Herzer, and D. Raabe, *Ultramicroscopy* (in press) doi: 10.1016/j.ultramic.2015.04.006.
- ⁵ K. Hono, D.H. Ping, M. Ohnuma, and H. Onodera, *Acta Mater.* **47**, 997 (1999).
- ⁶ K. Hono, *Prog. Mater. Sci.* **47**, 621 (2002).
- ⁷ G. Herzer, V. Budinsky, and C. Polak, *phys. stat. sol. B* **248**, 2382 (2011).
- ⁸ G. Herzer, *Mater. Sci. Eng. A* **181**, 876 (1994).
- ⁹ M. Ohnuma, K. Hono, T. Yanai, M. Nakano, H. Fukunaga, and Y. Yoshizawa, *Applied Physics Letters* **86**, 152513 (2005).
- ¹⁰ VITROPERM® 800, registered trademark of Vacuumschmelze GmbH & Co. KG.
- ¹¹ P. Midgley and R.E. Dunin-Borkowski, *Nature Materials* **8**, 271 (2009).
- ¹² G. Herzer, *IEEE Trans Magn* **25**, 3327 (1989).